NTHAS8: The Eighth Japan-Korea Symposium on Nuclear Thermal Hydraulics and Safety
Beppu, Japan, December 9-12, 2012

Paper Number N8P1081

STUDY ON BUBBLE BEHAVIOR OF INERT GASES AT ENTRANCE NOZZLE IN SODIUM-COOLED FAST REACTOR

Yuji Konaka[1*], Takashi Takata[1], Akira Yamaguchi[1], Kei Ito[2] and Hiroyuki Ohshima[2]

[1] Graduate School of Engineering, Osaka University
2-1 Yamadaoka, Suita, Osaka, Japan,565-0871
phone: +81-6-6879-7895; e-mail: konaka_y@qe.see.eng.osaka-u.ac.jp

[2] Japan Atomic Energy Agency
4002, Narita, O-arai, Higashi-Ibaraki, Ibaraki, Japan

ABSTRACT

Bubbles of inert gases exist in a primary coolant system of sodium-cooled fast reactor. Those bubbles may cause increase of reactivity in the core and cavitation erosion and so on. Therefore it is necessary from the viewpoint of reactor safety to understand the dynamic behavior of the bubbles. In this study, the model of gas transport at the entrance nozzle has been developed using a non – dimensional correlation based on a dynamic bubbles behavior. For this purpose, a three-dimensional analysis of dynamic bubbles behavior has been carried out by coupling one-way bubble tracking method with the multi-dimensional CFD tool, FLUENT. Then fractions of the bubbles out flowed through the entrance nozzle (f_{in}), accumulating under the core support plate (f_{res}) and dissolving in the liquid sodium (f_{dis}) are calculated. As a result, it has been demonstrated that f_{in} and f_{res} are influenced by the sodium flow field, bubble radius and the shape of the entrance nozzle, whereas f_{dis} is negligibly minimal. The authors have also developed a correlation for the gas behavior based on the dimensionless number which corresponds to the geometric, the buoyancy and the drag force effects acting on the bubble.

1. INTRODUCTION

Bubbles of inert gases exist in a primary coolant system of sodium-cooled fast reactor. The sources of the inert gases are argon used as cover gas at an upper plenum and helium released by B4C control rod material. These bubbles are transported according to the coolant flow in the primary system and may cause increase in reactivity in the core and a nucleation site for boiling and cavitation, flow instability, and an influence on heat transfer at the heat exchanger. Therefore it is essential from the perspective of reactor safety of the sodium-cooled fast reactor to understand the dynamics behavior of the bubbles exactly.

A computational code VIBUL for a dynamics of the bubbles in the primary coolant system had been originally developed for French fast reactor (Bertron, 1991) and modified for Japanese SFR design (Yamaguchi and Hashimoto, 2005). This code quantifies the amount of free bubbles and dissolved gas in sodium coolant. However, simple module models of bubble transport in each component are implemented and one-dimensional flow of models is assumed in the code. The simplification may not be sufficiently accurate to describe the bubble behavior especially in the complicated components such as an upper plenum of the reactor, an intermediate heat exchanger (IHX) and entrance nozzles at a high pressure plenum. It is essential to simulate bubble behavior in those complicated geometry and to estimate the amount of the gas bubbles and dissolved gas. Based on the computation, dominant factor for phenomena to the bubble behavior are identified and the non-dimensional correlations for the bubble behavior are developed. The VIBUL code is refined if the new correlations are included to take account for multi-dimensional flow and the bubble dynamics.

Consequently, the author has proposed the model of bubble transport at entrance nozzle based on theoretical and computational methods. For this purpose, a three-dimensional analysis of dynamic bubbles behavior has been carried out by using one-way babble tracking method which is specified to dilute two-phase flow. A commercial CFD tool, FLUENT (http://www.ansys.com /products/fluid-dynamics/fluent/) Ver. 6.3.26 is used in the analyses.

2. ONE-WAY BUBBLE TRACKING METHOD

In the one-way bubble tracking method, steady state flow field at entrance nozzle is computed first by using FLUENT. Then bubbles are tracked with the Lagrangian method and with the flow velocity field obtained from the flow field analysis.

2.1 Motion Equation of a Single Bubble

A motion equation with regard to a single bubble in a flow field is written as:

$$\frac{dV_b}{dt} = g\left(\frac{\rho_f - \rho_b}{\rho_b}\right) + \frac{3}{8r} C_D \frac{\rho_f}{\rho_b} \left|V_f - V_b\right| \left(V_f - V_b\right) \quad (1)$$

where V and g are velocity vector and the acceleration vector due to gravity. Subscripts b and f indicate bubble and flow phase, respectively. The first and the second terms of the right hand side of Eq. (1) are the buoyancy force and the drag force, respectively. Eq. (1) is integrated with the semi-implicit fourth-order Runge-Kutta method. C_D in Eq. (1) is the drag coefficient and is described as:

$$C_D = \frac{16}{Re_P} \qquad (Re_P < 10) \qquad (2)$$

$$C_D = \frac{18.7}{Re_p^{0.68}} \qquad (10 \le Re_P < 750) \qquad (3)$$

$$C_D = 0.44 \qquad (750 \le Re_P) \qquad (4)$$

where Re_P is the particle Reynolds number, which is the non-dimensional ratio of fluid inertial/convection forces to viscous forces with respect to fluid dynamics in the vicinity of the bubble. It is described as:

$$Re_p = \frac{2\rho_f \left|V_f - V_b\right| r}{\mu} \quad (5)$$

It is assumed that the influence of a bubble motion on the liquid phase is negligible because the bubble volume fraction is small enough. Therefore, one-way bubble tracking method is employed, in which the effect of bubble motion on flow field is not taken account, but only the effect of flow field on bubble motion.

2.2 Mass Conservation of a Single Bubble

A bubble shrinks or glows according to the mass transfer at the bubble-liquid interface. The mass conservation equation for a single bubble is written as:

$$\frac{dN_m}{dt} = -4k\pi r^2 \left[\frac{S \cdot \rho_f \cdot 10^{-5}}{M_f} \left(P_f + \frac{2\sigma}{r} \right) - N_d \right] \quad (6)$$

where N_m is moles of gas in a bubble, r is the radius of a bubble, P_f is the pressure in the liquid sodium, σ is the surface tension, N_d is the molar amount of dissolved gas included in a unit volume of liquid sodium, S is the solubility, ρ_f is the density of liquid sodium and M_f is the molar mass of liquid sodium. The solubility for noble gases such as argon and helium are given by Reed and Droher (1970). Eq. (6) is solved with the Eulerian explicit method. k is a mass transfer coefficient which is given by:

$$k = \frac{Sh \cdot D_{iff}}{2r} \quad (7)$$

where Sh is the Sherwood number , which is given by an experimental formula with particle Reynolds number and Schmidt number. D_{iff} is the diffusion coefficient of the gas in liquid sodium (Clift et al., 1978)

2.3 Interpolation between Bubble and Flow Field

The flow-phase velocity and pressure at the bubble's instantaneous position are used in Eq. (1) and (6). They are interpolated from the values at the several evaluation points located near the bubbles. These interpolations are carried out by the method used in MPS, Moving particle semi-implicit (Koshizuka, 2002). In this method, the data at the bubble's position is determined by the distance weighted average of values at the node points inside of the circle with effective radius as shown Fig. 1.

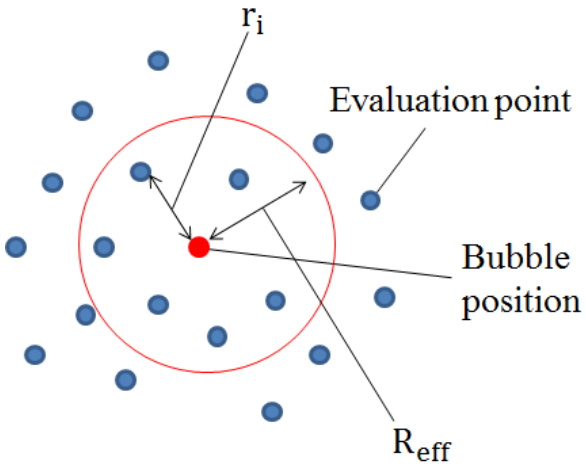

Fig. 1 Interpolation between bubble and flow field

This interpolation is defined in the following equation.

$$\varphi_f = \frac{\sum \varphi_i W(r_i)}{\sum W(r_i)} \quad (8)$$

where φ_f and φ_i are the flow-phase values at each bubble's position and at node points. $W(r_i)$ is weight coefficient and defined as:

$$W(r_i) = \begin{cases} \dfrac{R_{eff}}{r_i} - 1 & (r_i \le R_{eff}) \\ 0 & (r_i > R_{eff}) \end{cases} \quad (9)$$

where R_{eff} is effective radius and r_i is distance between a bubble and each node point.
It has been confirmed that this method reproduces the pressure and flow field at entrance nozzle with sufficient accuracy on R_{eff} =10mm.

3. NUMERICAL ANALYSIS OF ENTRANCE NOZZLE

3.1 Analytical Conditions

3.1.1 Flow Conditions

Three-dimensional analysis has been conducted under steady condition using FLUENT Ver. 6.3.26. Fig. 2 and Fig.3 shows the analytical model which is one-sixth of the plenum region taken up by an entrance nozzle because of the symmetry of the nozzle geometry.

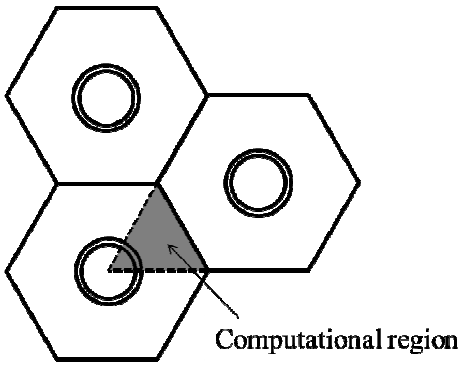

Fig. 2 Computational region in the high pressure plenum

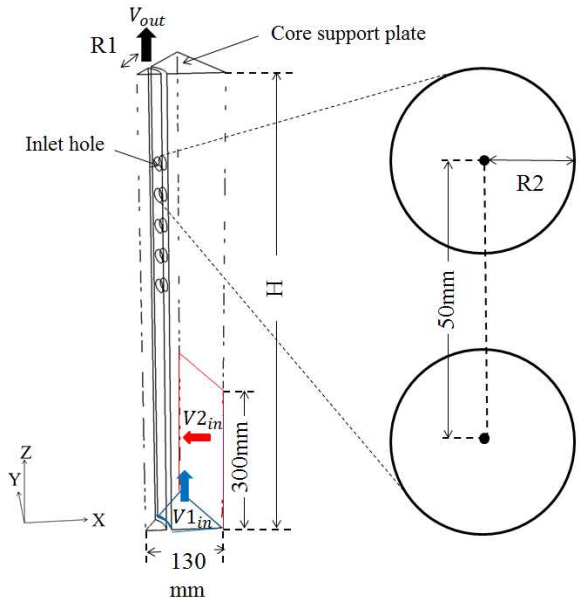

Fig. 3 Analytical model

The mesh arrangement, which is unstructured grid, is shown in Fig. 4. The number of meshes generated by GAMBIT 2.4.6 was about 100,000 meshes.

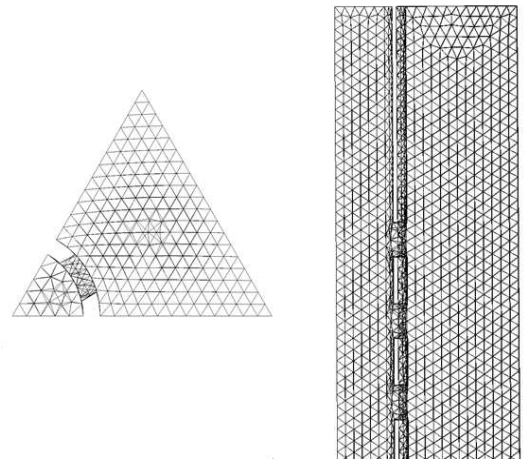

(a) plane view **(b) elevation view (upper part of model)**

Fig. 4 Mesh arrangement

In the analysis, the liquid sodium inlet is assumed in two ways, located at the bottom of the high pressure plenum ($V1_{in}$) and at the side of the model ($V2_{in}$) as shown in Fig. 3.
A parametric analysis is performed in order to estimate the influence of the model geometry and flow field on bubbles behavior. The selected parameters are following: the inlet velocity ($V1_{in}$, $V2_{in}$), the entrance nozzle radius (R1), the entrance nozzle length (H), the inlet hole radius (R2), the homothetic scale factor of the model and the number of inlet holes (N_{hole}).
Each geometric parameter is varied as displayed in Table 1. Fig. 5 shows how to change the number of inlet holes.

Table 1 Geometric parameter

parameter		**Base case**		
R1 (mm)		**35.5**	50.0	70.0
R2 (mm)	7.0	**11.0**	15.0	
H (mm)	684	**784**	884	
Scale (-)	0.50	**1.00**	2.00	
The number of inlet hole	3	**5**	7	

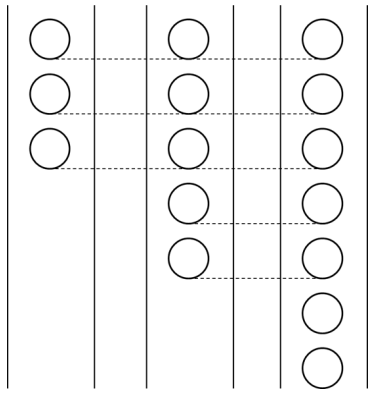

(a) 3holes (b) 5holes (c) 7holes

Fig. 5 Location of inlet holes

In the parametric analysis, the inlet flow velocity ($V1_{in}$, $V2_{in}$) was determined based on both conditions consistent mass flow rate and consistent inlet velocity. Table 2 shows the inlet flow velocity in the case of mass flow rate consistent conditions.

Table 2 Inlet flow velocity (Mass flow rate consistent conditions)

Output power (%)			100	50	10
Mass flow rate (kg/s)			3.34	1.67	0.33
Inlet Velocity (m/s)	$V2_{in}$	R1=35.5 mm	0.10	0.05	0.01
	$V1_{in}$ (BASE)	R1=35.5 mm	0.62	0.31	0.06
		R1=50.0 mm	0.71	0.35	0.07
		R1=70.0 mm	0.95	0.48	0.10

The temperature in the high pressure plenum is 668K. Although the dissolution of bubbles is related to the initial molar concentration of the dissolved gas, no initial dissolution is assumed for simplicity because of the rarity. Also, since the argon gas is the most significant source, the helium gas is not considered.

3.1.2 Bubble Conditions

When a bubble passes the primary pump or fuel subassemblies where liquid sodium flows at high velocity and turbulence is significant, a large bubble breaks up by the shear force. The shear force is related to the velocity differential at a distance of bubble diameter. It is known that a bubble breaks up in a flow field when the Weber number (*We*) is greater than the critical Weber number (We_c) of 4.7 (Lewis and Davidson, 1982). Then the maximum radius is given to be 297μm disintegration in the Super Phenix design condition (Mignot, 1978). Since a bubble density is thin in the primary cooling system, bubble coalescence is negligible. Therefore, a bubble larger than 297μm in radius does not exist in the system. The inner pressure of a bubble increases significantly due to surface tension in accordance with the decrease of bubble radius. Consequently, a tiny bubble dissolves immediately. In the previous study of the gas dynamics analysis (Yamaguchi and Hashimoto, 2005), it was found that most of the bubbles existed in the range of 10 - 80μm. Hence we select 1μm and 297μm as the minimum and the maximum radius, respectively. The initial bubble radius is discretized into fifty radius groups ranging from 1μm to 297μm as followings.

$$r_i = r_{\min} \times 10^{k(i-1)} \qquad (10)$$

where r_i is bubble radius and *k* is described as:

$$k = \frac{1}{(50-1)} log_{10} \frac{r_{\max}}{r_{\min}} \qquad (11)$$

200 bubbles from each of radius groups are randomly placed at the cross section (Z=200mm) out of an entrance nozzle in each computation (in total, 10000 bubbles in one case).
The variable time step, which is set that the distance bubble moving at a step is constant, is applied in the computation. The constant distance (ΔS) is stated as 0.1mm.
Some bubbles in the high pressure plenum are conveyed by the liquid sodium flow and enter inlet holes of entrance nozzles and go to reactor core. Others staying in the plenum may dissolve and disappear in the liquid sodium. The rest of bubbles broach and accumulate under a core support plate. The calculation is stopped when all bubbles get the any state of the following: entering reactor core, completely dissolved and reaching a core support plate.

3.2 Results and Discussions

3.2.1 BASE case

Figure 6 shows the stream lines of the flow velocity in 100% output power for the cases of flow inlet located at the bottom and at the side. As seen in Fig. 6, They have a similar in flow distribution near the entrance nozzle. The flow velocity in upper inlet holes is larger than in lower ones. With this result, it is easy expected that upper inlet holes suck more bubbles than lower ones.

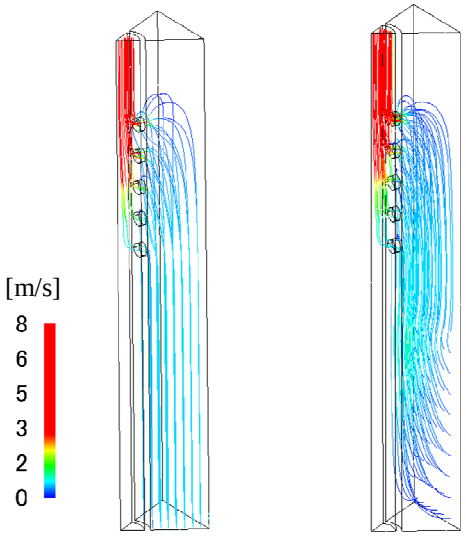

Fig. 6 100% mass flow rate stream line

The mass fractions of the bubbles flowing into reactor core through the inlet hole (f_{in}), accumulating under a core support plate (f_{res}) and dissolving in the liquid sodium (f_{dis}) are calculated. The three quantities are summed up to unity. Fig. 7 shows the residual bubbles fraction (f_{res}) as a function of the initial bubble radius. It can be seen from this figure that there is no great difference between the bottom inlet condition and the side inlet condition. Also, the residual fraction is the largest for large bubbles and in slow flow field.

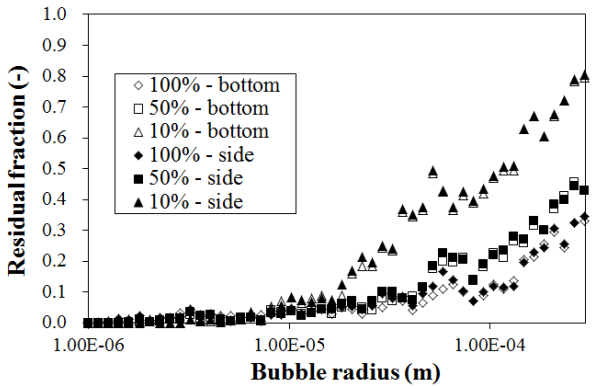

Fig. 7 Residual fraction

The dissolution fraction in the case of bottom inlet condition is indicated in Fig. 8. The smaller bubbles have the higher dissolution fraction due to the high surface tension. The dissolution fraction increases as flow velocity becomes low. This is attributed to the fact that the bubbles tend to stay for a long time in the analytical region. However, since the high pressure plenum is at a relatively-low temperature 668K, the dissolution fraction is negligibly minimal as shown in Fig.8.

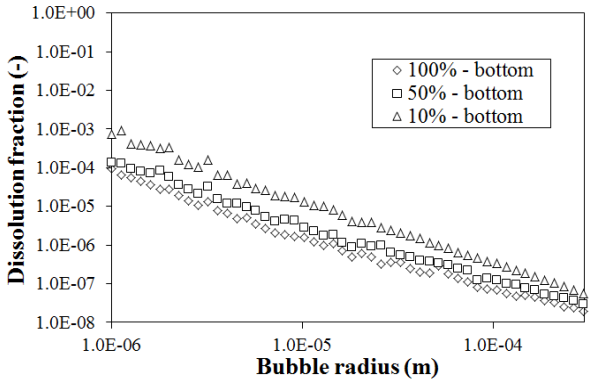

Fig. 8 Dissolution fraction

As a result of analyses in BASE case, it is found that bubbles behavior depends on the initial bubble radius and flow field. Furthermore, this analytical result has been addressed by using the dimensionless number with regard to a bubble behavior in order to clarify the relationship between bubbles behavior and bubble and flow conditions. In this analysis, the drag force, which makes bubbles go with the flow, and the buoyancy force are chosen as influencing factors. The dimensionless number which is the proportion of buoyancy force and drag force is as followings:

$$\frac{F_b}{F_d} = \frac{g\left(\frac{\rho_f - \rho_b}{\rho_b}\right)}{\frac{3}{8r} C_D \frac{\rho_f}{\rho_b}\left(V_f - V_b\right)^2} = \frac{g\left(\frac{\rho_f - \rho_b}{\rho_b}\right)}{\frac{3}{8r} C_D \frac{\rho_f}{\rho_b} V1_{in}{}^2} \qquad (12)$$

where F_b is buoyancy force and F_d is drag force. The inlet velocity ($V1_{in}$), which means the superficial velocity is chosen as the characteristic velocity. The correlation between each fraction and F_b / F_d is shown in Fig. 9. This indicates that the dimensionless number which correspond to the buoyancy and the drag force effects acting on the bubble have a dominant influence on bubbles behavior at the entrance nozzle under the BASE case.

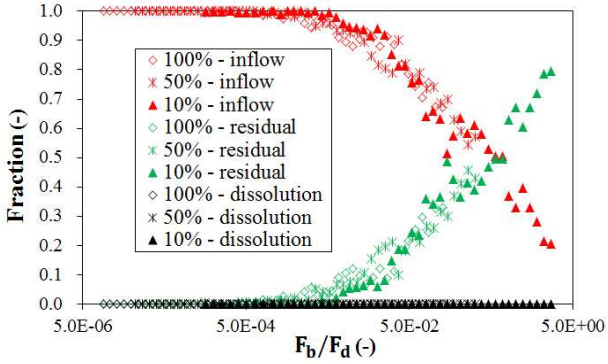

Fig. 9 Non-dimensional correlation (BASE case)

3.2.2 Geometric effect

Parametric analyses regarding geometry have been conducted in order to estimate the effect of the entrance nozzle geometry on the bubbles behavior.

Figure 10 shows the influence of the number of inlet holes on inflow fraction of bubbles. It is mentioned that the number of inlet holes on the entrance nozzle has little influence on bubbles behavior at the entrance nozzle. On the other hand, Fig. 11 shows the relationships between the rate of bubbles inflowing into each inlet hole and the location number of the inlet hole, which is arranged in ascending order from the upper position. It is shown that inlet holes located in the upper part have larger suction force than ones in the bottom part. Hence, it is noted that the most of inflowing bubbles inflow into upper inlet holes which have large suction even if the number of inlet holes is small. This is why bubbles behavior is hardly affected by the number of inlet holes. Furthermore, It is also noted that the relationship between attractive force of each inlet hole depends on the relationship between inflow velocities in each inlet hole as shown in Fig. 12.

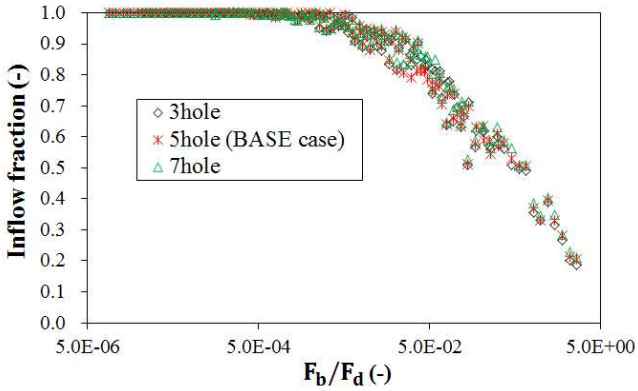

Fig. 10 Influence of the number of inlet hole

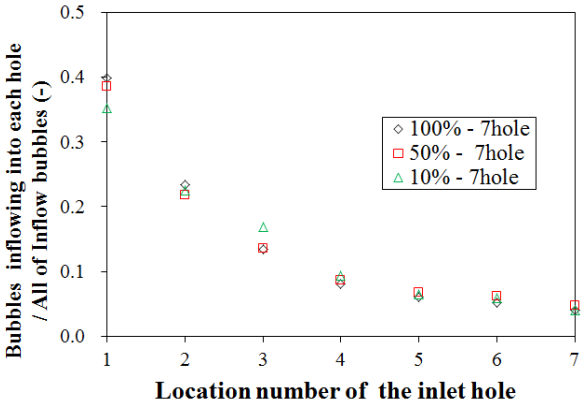

Fig. 11 Rate of bubbles inflowing into each inlet hole

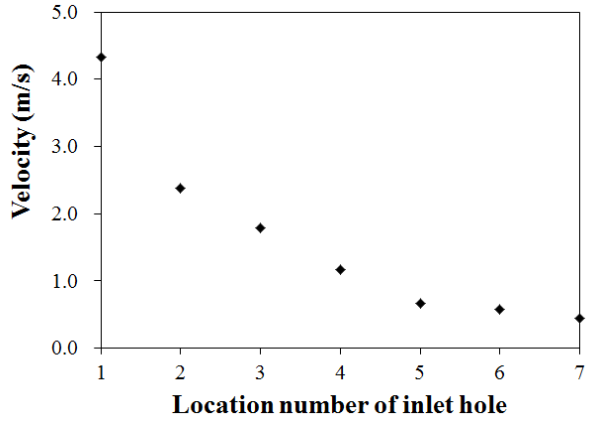

Fig. 12 Velocity in each inlet hole

Figure 13 shows the influence of the entrance nozzle radius, the entrance nozzle length, inlet hole radius and the homothetic scale factor on the inflow fraction (f_{in}), respectively. As shown in them, bubbles behavior at the entrance nozzle is little-affected by the change of geometry.

It is found that the geometric effect on bubbles behavior at the entrance nozzle is much lesser than the buoyancy and drag force effects and negligibly small within the range of the geometric parameters in this paper.

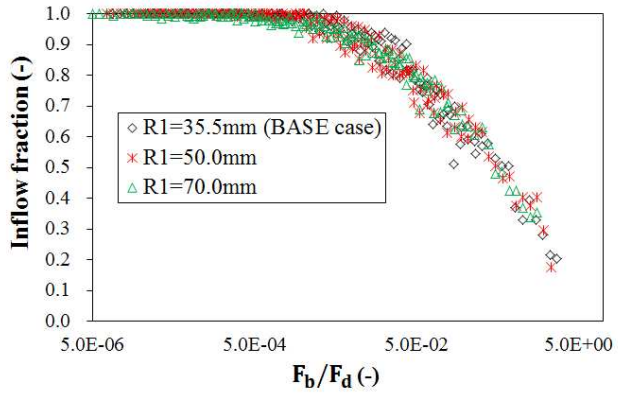

(a) Entrance nozzle radius

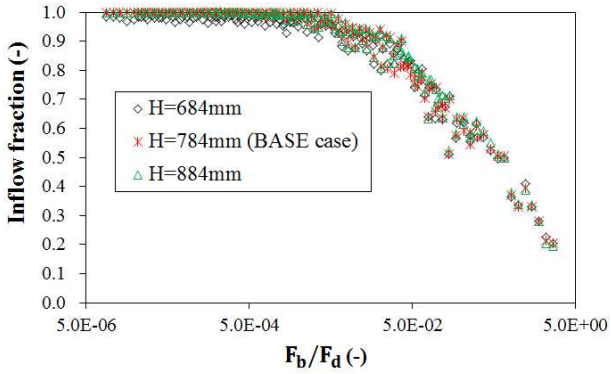

(b) Entrance nozzle length

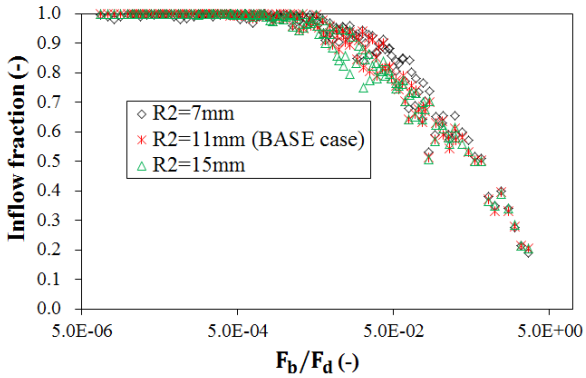

(c) Inlet hole radius

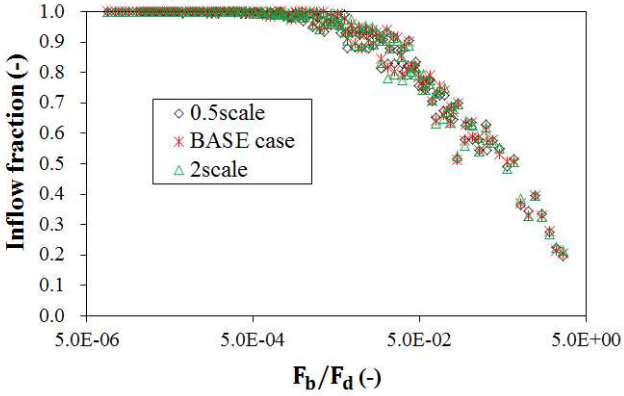

(d) Homothetic scale factor

Fig. 13 Geometric effect

We have proposed the model of bubbles behavior at the entrance nozzle using the dimensionless correlation which takes multi-dimensional effect on bubbles into consideration. It can be seen that the inflow fraction (f_{in}) is excellently expressed as shown in Fig. 14. The function of the non-dimensional correlation is expressed as:

$$f_{in} = \exp\left\{0.0769\left(\frac{F_b}{F_d}\right) - 1.0789\sqrt{\frac{F_b}{F_d}} + 0.0147\right\} \quad (13)$$

$$R^2 = 0.9698$$

where R^2 is correlation coefficient. Furthermore, because the dissolution of bubbles is negligibly-small as noted in the previous chapter, residual and dissolution

fractions are described as shown as below.

$$f_{res} = 1 - f_{in} \quad (14)$$

$$f_{dis} = 0 \quad (15)$$

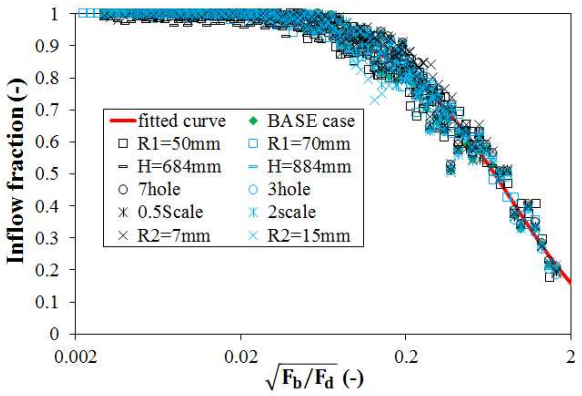

Fig.14 Non-dimensional correlation for inflow fraction

4. CONCLUSIONS

A multi-dimensional flow simulation at the entrance nozzle has been carried out using a commercial CDF tool, FLUENT Ver. 6.3.26.

A bubbles behavior analysis at the entrance nozzle coupled with multi-dimensional flow field by using one-way bubble tracking method.

As a result of the analyses, it is found that bubbles behavior depends on the bubble radius and the flow field at the entrance nozzle. On the other hand, the gas dissolution is negligible because of a relatively-low temperature in the high pressure plenum.

It is also demonstrated that bubbles behavior at the entrance nozzle is dominantly influenced by the dimensionless number which represent the balance of drag force and buoyancy force acting on a bubble and hardly affected by the geometry effects within the range of the parameters in this paper.

A non-dimensional correlation for the bubbles behavior at the entrance nozzle has been derived and the new model has been proposed of the bubbles behavior at the entrance nozzle which takes multi-dimensional effects on bubbles behavior into consideration.

NOMENCLATURE

r	Radius	[m]
V	Velocity	[m/s]
V_{in}	Inlet Velocity	[m/s]
C_D	Drag coefficient	[-]
g	Acceleration due to gravity	[m/s^2]
N_m	Molar amount of a gas in a bubble	[mol]
k	Mass transfer coefficient	[m/s]
S	Solubility	[Pa^{-1}]
M	Molar mass	[kg]
P	Pressure	[Pa]
Sh	Sherwood number	[-]
N_d	Molar amount of dissolved gas in a unit volume of sodium	[mol/m^3]
D_{iff}	Diffusion coefficient	[-]
W	Weight coefficient	[-]
R_{eff}	Effective radius	[m]
$R1$	Entrance nozzle radius	[m]
$R2$	Inlet hole radius	[m]
H	Entrance nozzle length	[m]
f_{in}	Inlet fraction	[-]
f_{res}	Residual fraction	[-]
f_{dis}	Dissolution fraction	[-]
F_d	Drag force	[N]
F_b	Buoyancy force	[N]

Greek Letters

ρ	Density	[kg/m^3]
μ	Coefficient of viscosity	[Pa·s]
σ	Surface tension	[N/m]
φ	Physical quantity	[-]

Subscripts

b	Bubble phase
f	Fluid phase

REFERENCES

Clift, R, J., R.Grace and M.E.Weber (1978). "Bubbles, Drops and Particles," *Academic Press*

Koshizuka, S. (2002) "Numerical Analysis of Flow using Particle Method," *Flow21*, 230-239

Mignot, G. (1997) " Modèle de désorption nuclée dans les échangeurs intermédiaries d'un réacteur àneutrons rapides," *NTCEA/SER/LETH97/5016*

Reed, E.L. and Dropher,J.J. (1970). "Solubility and Diffusivity of inert gases in liquid sodium, potassium and NaK," *Liquid Metal Engineering Center Report* LMEC-69-36

Tatsumi, E. et al. (2006) "Numerical study on dissolved gas and bubble behavior in fluid" *fifth Japan-Korea Symposium on Nuclear Thermal Hydraulics and Safety* (NTHAS-5), F005, Jeju, Korea, Nov. 26-29.

Yamaguchi, A. and Hashimoto, A. (2005). "A Computational Model for Dissolved Gas and Bubble Behavior in the Primary Coolant System of Sodium-Cooled Fast Reactor," 11th International Topical Meeting on Nuclear Reactor Thermal-Hydraulics, France, October, 2005, 477